Letter

Nuclear density dependence of polarization transfer in quasi-elastic $A(\vec{e}, e'\vec{p})$ reactions

T. Kolar,[1,*] W. Cosyn,[2] C. Giusti,[3] P. Achenbach,[4,†] A. Ashkenazi,[1] R. Böhm,[4] D. Bosnar,[5] T. Brecelj,[6] M. Christmann,[4] E. O. Cohen,[1,‡] M. O. Distler,[4] L. Doria,[4] P. Eckert,[4] A. Esser,[4] J. Geimer,[4] R. Gilman,[7] P. Gülker,[4] M. Hoek,[4] D. Izraeli,[1] S. Kegel,[4] P. Klag,[4] I. Korover,[1,§] J. Lichtenstadt,[1] M. Littich,[4] T. Manoussos,[4] I. Mardor,[1,8] D. Markus,[4] H. Merkel,[4] M. Mihovilovič,[9,6,4] J. Müller,[4] U. Müller,[4] M. Olivenboim,[1] J. Pätschke,[4] S. J. Paul,[10] E. Piasetzky,[1] S. Plura,[4] J. Pochodzalla,[4] M. Požun,[6] G. Ron,[11] B. S. Schlimme,[4] M. Schoth,[4] F. Schulz,[4] C. Sfienti,[4] S. Širca,[9,6] R. Spreckels,[4] S. Štajner,[6] S. Stengel,[4] E. Stephan,[12] Y. Stöttinger,[4] S. Strauch,[13] C. Szyszka,[4] M. Thiel,[4] A. Weber,[4] A. Wilczek,[12] and I. Yaron[1]
(A1 Collaboration)

[1]*School of Physics and Astronomy, Tel Aviv University, Tel Aviv 69978, Israel*
[2]*Florida International University, Miami, Florida 33199, USA*
[3]*INFN, Sezione di Pavia, via A. Bassi 6, I-27100 Pavia, Italy*
[4]*Institut für Kernphysik, Johannes Gutenberg-Universität, 55099 Mainz, Germany*
[5]*Department of Physics, Faculty of Science, University of Zagreb, HR-10000 Zagreb, Croatia*
[6]*Jožef Stefan Institute, 1000 Ljubljana, Slovenia*
[7]*Rutgers, The State University of New Jersey, Piscataway, New Jersey 08855, USA*
[8]*Soreq NRC, Yavne 81800, Israel*
[9]*Faculty of Mathematics and Physics, University of Ljubljana, 1000 Ljubljana, Slovenia*
[10]*Department of Physics and Astronomy, University of California, Riverside, California 92521, USA*
[11]*Racah Institute of Physics, Hebrew University of Jerusalem, Jerusalem 91904, Israel*
[12]*Institute of Physics, University of Silesia in Katowice, 41-500 Chorzów, Poland*
[13]*University of South Carolina, Columbia, South Carolina 29208, USA*

(Received 2 April 2024; accepted 27 November 2024; published 12 December 2024)

The ratio of the transverse and longitudinal components of polarization transfer to protons in the quasielastic $(\vec{e}, e'\vec{p}\,)$ reaction, P'_x/P'_z, is sensitive to the proton's electromagnetic form factor ratio, G_E/G_M. To explore density-dependent in-medium modifications, a comparison of polarization transfer ratios involving protons from distinct nuclear shells, each with different local nuclear densities, has been proposed. In this study, we present such comparisons between four shells, $1s_{1/2}$, $1p_{3/2}$ in ^{12}C and $1d_{3/2}$, $2s_{1/2}$ in ^{40}Ca. In an effort to account for other many-body effects that may differ between shells, we use a state-of-the-art relativistic distorted-wave impulse-approximation (RDWIA) calculation and present the double ratios $(P'_x/P'_z)_{\mathrm{Data}}/(P'_x/P'_z)_{\mathrm{RDWIA}}$ as well as the super-ratios $[(P'_x/P'_z)_{\mathrm{A}}/(P'_x/P'_z)_{\mathrm{B}}]_{\mathrm{Data}}/[(P'_x/P'_z)_{\mathrm{A}}/(P'_x/P'_z)_{\mathrm{B}}]_{\mathrm{RDWIA}}$, for chosen shells A and B, as a function of effective local nuclear densities. We find that double ratios for individual shells show a dependence on the probed effective nuclear densities. Studying the super-ratios, we observed a systematic variation between pairs of higher- and lower-density shells.

DOI: 10.1103/PhysRevC.110.L061302

Introduction. Polarization transfer to a proton bound in a nucleus has been suggested as a tool to observe in-medium modifications in the bound proton structure [1]. It is a part of a wider effort to understand the role of quarks and gluons in nuclei [2]. Some calculations introduce in-medium modifications and suggest nuclear-density-dependent changes of the bound nucleon electromagnetic (EM) form factors (FFs) [3–5]. We report on the first systematic search for nuclear density-dependent effects in the quasielastic $A(\vec{e}, e'\vec{p})$ reaction, which is sensitive to EM FFs.

For a free proton, the ratio of the transverse and longitudinal polarization-transfer components, P'_x/P'_z, in polarized elastic electron scattering, under the one-photon exchange approximation, is proportional to the proton EM form-factor ratio, G_E/G_M. Similarly, a polarization transfer in the quasielastic $A(\vec{e}, e'\vec{p}\,)$ reaction is sensitive to the *effective* EM FFs, which are related to the charge and magnetization distributions of the bound proton. However, quasielastic reactions are subject to other many-body effects, such as final state interactions, isobar configurations, and meson-exchange currents, which need to be well understood in order to isolate possible deviations due to modifications in the proton structure.

It has been suggested to study the *double ratios* [5], $(P'_x/P'_z)_{\mathrm{Data}}/(P'_x/P'_z)_{\mathrm{Calc}}$, thus dividing out the nuclear

*Contact author: tkolar@mail.tau.ac.il
†Present address: Thomas Jefferson National Accelerator Facility, Newport News, VA 23606, USA.
‡Also at Soreq NRC, Yavne 81800, Israel.
§Also at Department of Physics, NRCN, P.O. Box 9001, Beer-Sheva 84190, Israel.

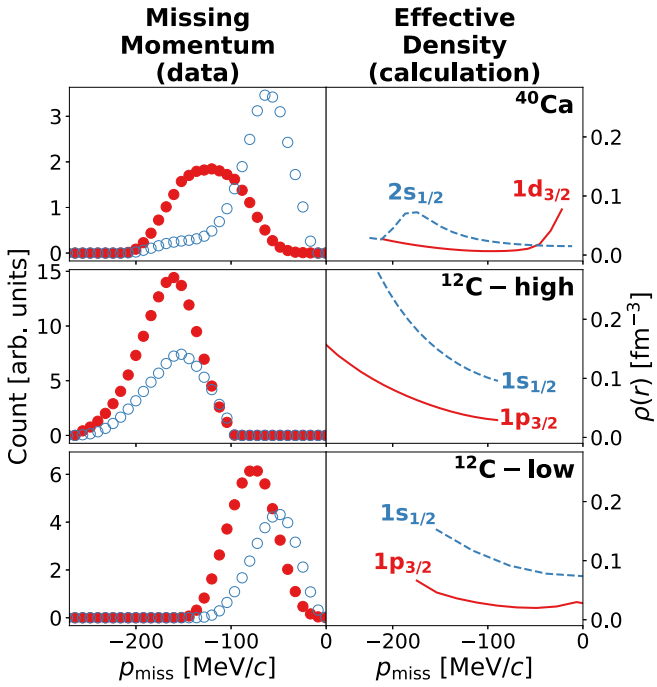

FIG. 1. Measured missing momentum distribution (left) and effective local nuclear densities (right) calculated in RDWIA for the three kinematic settings from Table I.

many-body effects included in the calculation. Furthermore, pairs of different shells (shell A and B), characterized by different nuclear densities, can be compared by the *super-ratios* $[(P'_x/P'_z)_A/(P'_x/P'_z)_B]_{Data}/[(P'_x/P'_z)_A/(P'_x/P'_z)_B]_{Calc}$, looking for density-dependent medium modifications. The super-ratios account for those differences in many-body effects that are included in the model, and reduce the sensitivity to systematic discrepancies common to calculations for different shells.

Density-dependent modifications are expected to be at the level of a few percent [5], which requires high statistical accuracy. ^{12}C was suggested as a good nucleus for such studies since the effective local nuclear density experienced by the protons bound in the $1s_{1/2}$ shell is about twice the density for those in the $1p_{3/2}$ shell. Comparison of polarization ratios for protons from $1s_{1/2}$ and $1p_{1/2}$ shells in ^{12}C has shown that the p to s double ratio was 1.15 ± 0.03 [6]. Relativistic distorted-wave impulse-approximation (RDWIA) calculations only partially accounted for this deviation from unity, while the relativistic plane-wave impulse-approximation (RPWIA) did not predict this difference. However, once protons were compared at the same virtuality, the results became consistent with unity, 1.05 ± 0.05, and so did RPWIA and RDWIA calculations [6]. We note that, as seen in Fig. 2 of Ref. [6], in the virtuality overlap region, we are effectively comparing the low-p_{miss} region of $1s_{1/2}$ to the high-p_{miss} region of $1p_{3/2}$. This reduces the difference in the probed effective densities between the two shells (see Fig. 1).

In this work we reanalyze recent data obtained for protons from the $1d_{3/2}$ and $2s_{1/2}$ shells in ^{40}Ca [7] and $1s_{1/2}$ and $1p_{1/2}$ shells in ^{12}C under two different kinematic settings [6,8]. We compare the experimentally obtained ratios of polarization transfer components with corresponding RDWIA calculations, and preform the first systematic search for nuclear density-dependent effects in $A(\vec{e}, e'\vec{p})$.

TABLE I. Kinematic settings of the $A(\vec{e}, e'\vec{p})$ measurements considered in this work. Following the beam energy, E_{beam}, and the square of the transferred four-momentum, Q^2, we list the missing momentum ranges covered and its average for each considered shell. For p_e and θ_e (p_p and θ_p) we denote the scattered electron (knocked-out proton) central momentum and angle settings, respectively.

Kinematic setting		^{12}C-low	^{12}C-high	^{40}Ca
E_{beam}	(MeV)	600	600	600
Q^2	[(GeV/c)^2]	0.40	0.18	0.25
p_{miss}	(MeV/c)	$[-150, 0]$	$[-260, -100]$	$[-210, -17]$
$\langle p_{miss} \rangle$	(MeV/c)	$1p_{3/2}$: -82	$1p_{3/2}$: -171	$1d_{3/2}$: -123
		$1s_{1/2}$: -60	$1s_{1/2}$: -161	$2s_{1/2}$: -72
p_e	(MeV/c)	384	368	396
θ_e	(deg)	82.4	52.9	61.8
p_p	(MeV/c)	668	665	630
θ_p	(deg)	34.7	37.8	40.2

Polarization transfer data. The polarization transfer components from the quasielastic $A(\vec{e}, e'\vec{p})$ reaction on ^{12}C and ^{40}Ca were measured at the three-spectrometer facility of the A1 Collaboration at the Mainz Microtron (MAMI), using the 600 MeV polarized continuous-wave electron beam. The scattered electrons and the knocked-out protons were detected in coincidence using two magnetic spectrometers. The polarization components were measured with a polarimeter located near the focal plane of the proton spectrometer. These measurements were reported in Refs. [6–8], and their kinematic parameters are summarized in Table I. We follow [6] and define the scalar proton missing momentum $p_{miss} \equiv \pm|\vec{p}_{miss}| = \pm|\vec{q} - \vec{p}'|$, where $\vec{q}$ and $\vec{p}$ are the momentum transfer and the outgoing proton momentum, respectively. The sign is taken to be positive (negative) if the longitudinal component of $\vec{p}_{miss}$ is parallel (antiparallel) to $\vec{q}$.

The ^{12}C data sets cover two ranges in p_{miss}: the low-p_{miss} setting is centered around $p_{miss} = 0$ MeV/c and extends to $p_{miss} = \pm 140$ MeV/c, while the high-p_{miss} data range from -260 to -100 MeV/c. The data obtained for ^{40}Ca span the range of $-200 < p_{miss} < -20$ MeV/c. The shell from which the proton was ejected was determined from the missing energy of each event. The measured missing momentum spectrum for each data set is shown in the left column of Fig. 1.

Calculation of the polarization transfer. The polarization transfer for each data set was calculated with the RDWIA model of Ref. [9] using free-proton EM form factors. Our previous analyses have shown that the calculated results are in good agreement with the measured polarization transfer data [6–8].

The calculations were performed on an event-by-event basis. Using each event's kinematics parameters ensures a full match of the calculation to the experimental kinematics acceptance. It also allowed us to extract per-bin averages of the calculated observables. The original RDWIA program [9] was modified to include all 18 hadronic structure functions for the $A(\vec{e}, e'\vec{p})$ reaction in the Born approximation

[10]. The RDWIA calculations use the global democratic relativistic optical potential [11], relativistic bound-state wave functions obtained with the NL-SH parametrization [12], and free-proton EM FFs using the Bernauer parametrization [13].

These calculations were compared to the measured polarization transfer data. More details are available in Refs. [6–8,14,15]. The impact of deficiencies in the calculations can be further reduced by studying the ratios, P'_x/P'_z, rather than the individual components, P'_x and P'_z. The double ratio, $(P'_x/P'_z)_{\rm Data}/(P'_x/P'_z)_{\rm RDWIA}$, factors out the many-body effects in the quasielastic process which are accounted for in the calculation. We note that in parallel/antiparallel kinematics the calculations depend linearly on the proton EM FFs ratio [7].

Effective nuclear densities. The effective local densities for protons removed from different shells in ^{12}C and ^{40}Ca have been obtained by following the procedure described in Refs. [5,16] but in RDWIA using the same model discussed above. In RDWIA the $(e, e'p)$ cross section is not factorized and the distorted momentum distribution from [16] corresponds to the so-called reduced cross section [9,10]. The reduced cross section is obtained by dividing the cross section by a kinematical factor and the elementary off-shell electron-proton scattering cross section, for which we used the cc2 prescription of de Forest [17]. This way we obtain a spectral-function-like dependence solely on $E_{\rm miss}$ and $p_{\rm miss}$, but with included FSI and other many-body effects. We note that in the nonrelativistic PWIA the reduced cross section gives the momentum distribution of the bound proton wave function and, in a factorized DWIA, the so-called distorted momentum distribution.

The calculated effective densities are shown in Fig. 1 (right). We note the large differences between the effective densities of the s and p shells in ^{12}C. Similar differences were predicted in Ref. [5] and suggested for studies of in-medium effects on the bound proton structure. The effective local densities in the s and d shells of ^{40}Ca are similar, thus differences between these shells are expected to be smaller. A comparison of a shell in ^{12}C with a shell in ^{40}Ca can serve as a cross-check to density-dependent modifications, but it is more susceptible to systematic uncertainties and deficiencies in the calculations.

Density dependence of the polarization transfer: Single-shell comparison with RDWIA. In parallel and antiparallel quasielastic kinematics and in the one-photon exchange approximation, the calculated P'_x/P'_z ratios depend linearly on G_E/G_M, which is the case for the data used in this work. The single-shell double ratios between the measured polarization transfer and those calculated in RDWIA with free-proton form factors, $(P'_x/P'_z)_{\rm Data}/(P'_x/P'_z)_{\rm RDWIA}$, are shown in Fig. 2 as a function of the effective local nuclear density (Fig. 1). These values were obtained as a weighted average over several $p_{\rm miss}$ bins for a better comparison between experimental and theoretical results over the kinematic phase space.

The double-ratio results indicate a statistically significant linear decrease as a function of the effective nuclear density with a slope of (-0.59 ± 0.16) fm^3. At $\overline{\rho} = 0$, the fit has a value of 1.066 ± 0.015, where it is expected to be unity. This can be explained by the 2% systematic uncertainties of the

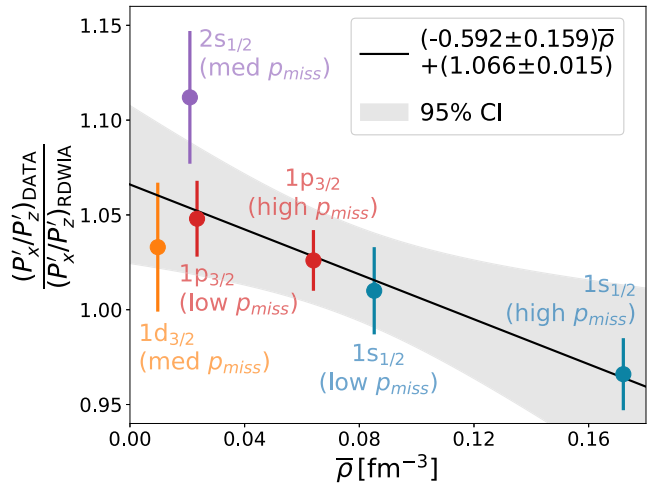

FIG. 2. Single-shell double ratios between the measured polarization transfer components and the ones calculated with the RDWIA model from [9] as a function of the effective local nuclear density. From the fitted linear function and its 95% confidence level band, a clear signature of a density-dependent effect with a negative slope can be seen.

data [6–8], and possible deficiencies in the models which may systematically underestimate the data. We check the consistency of these data with a proposed reduction of the effective G_E/G_M ratio [5] in the last section of this paper. Nevertheless, discrepancies at the level of a few percent are not necessarily a consequence of in-medium modifications. We cannot rule out RDWIA deficiencies (non-density-dependent) that might contribute to the observed slope. To reduce effects of such possible deficiencies we study also the super-ratios presented bellow.

Two-shell comparison with RDWIA. Kinematic variations may affect the double ratio between two shells, A and B, $(P'_x/P'_z)_{\rm A}/(P'_x/P'_z)_{\rm B}$. In addition, many-body effects like FSI may be different for different shells. Those considered in the model can be largely factored out by dividing the experimental double ratio by the calculated one. Furthermore, any theoretical discrepancies common to various shells would also cancel. Thus, the *super-ratio*,

$$\mathcal{R}_{\rm D} = \frac{[(P'_x/P'_z)_{\rm A}/(P'_x/P'_z)_{\rm B}]_{\rm Data}}{[(P'_x/P'_z)_{\rm A}/(P'_x/P'_z)_{\rm B}]_{\rm RDWIA}}, \qquad (1)$$

is expected to have an improved sensitivity to the bound proton properties over other many-body effects. It allows a better comparison between a free and a bound proton. Because the calculations are performed using the elastic proton FFs, the super-ratio provides a measure of the relative deviation of the effective FF ratio in the two shells.

Since medium modifications are expected to be small, at a few percent level [5], a measurement in a single configuration may not have sufficient statistical precision to observe such effects. However, the various measurements carried over different regions of $p_{\rm miss}$ and nuclei, probing different effective local nuclear densities, allow us to do a systematic study of the super-ratios. Each measurement is characterized by

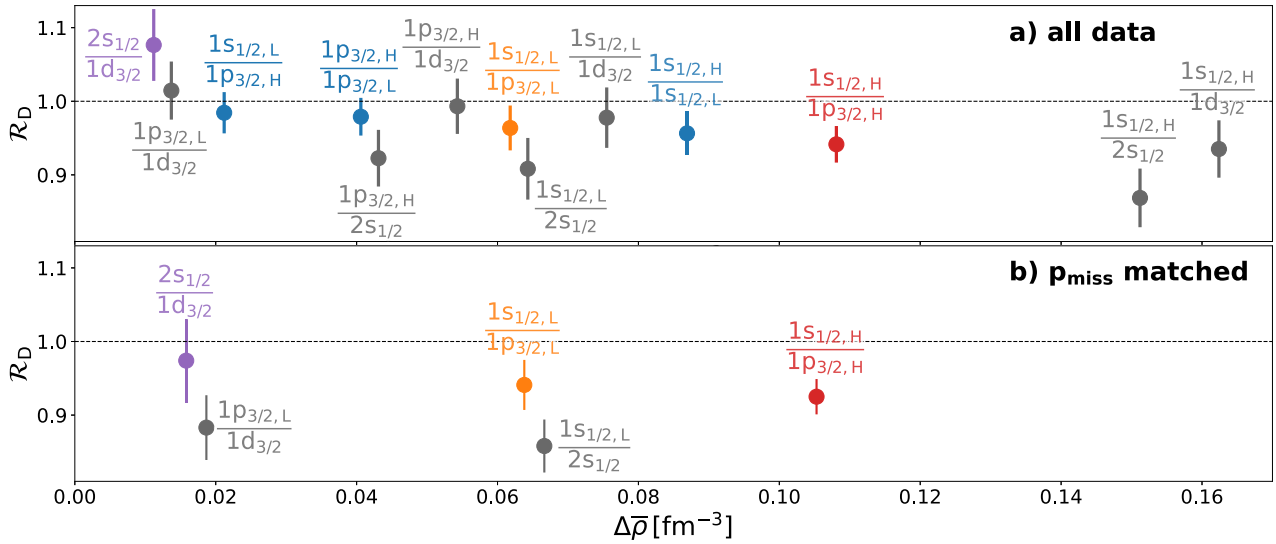

FIG. 3. The super-ratio from Eq. (1) as a function of density difference between the two shells. The ratios are constructed with denser shell being always in the numerator of measured and calculated double ratios. Ratios between shells of the same nucleus are shown in color, while those formed for shells across the two nuclei are shown in gray. Subscripts H and L next to ^{12}C shells denote high- and low-p_{miss} settings, respectively.

different effective nuclear densities (see Fig. 1). In Fig. 3(a) we show super-ratios comparison of higher- to lower-density shells as a function of the *difference* in the probed density. The *super-ratios* are shown for two measurements on $1s_{1/2}$ and $1p_{3/2}$ protons in ^{12}C, covering low- and high-p_{miss} ranges, and for a measurement of $2s_{1/2}$ and $1d_{3/2}$ protons in ^{40}Ca (see Table I).

As inferred from the negative slope of the linear density dependence of the ratios shown in Fig. 2, the super-ratios are on average below unity and tend to decrease with increasing density difference. We observe in Fig. 1 that between the $1s_{1/2}$ and $1p_{3/2}$ shells in ^{12}C the density differs progressively with increase of p_{miss}. The densities of the $2s_{1/2}$ and $1d_{3/2}$ shells in ^{40}Ca stay much closer over the measured p_{miss} range. Accordingly, we observed deviations in the ratios between ^{12}C shells being larger at high p_{miss} than at low p_{miss} and almost no effect present in the ratio between the s and d shells in ^{40}Ca, where densities are comparable. This suggests the presence of a density-dependent effect not yet included in RDWIA calculations.

We also present super-ratios from specific shells for different nuclei: the $1s_{1/2}$ ($1p_{3/2}$) protons in ^{12}C to those from $2s_{1/2}$ ($1d_{3/2}$) in ^{40}Ca to probe the high (low) density difference. These *cross-nuclei ratios* shown in Fig. 3 are more likely to be influenced by systematic uncertainties in either measurements or calculations. Nevertheless, we see that almost all of them fall below unity and are consistent with ratios between shells of the same nucleus.

In Fig. 3(b) we present the same super-ratios as in Fig. 3(a), but we consider only data from overlapping regions of p_{miss} distributions of the compared shells. The overlap region was first subdivided into several bins before obtaining the super-ratios and subsequently taking their weighted average. This differs from data shown in Fig. 3(a), where the super-ratio was formed from weighted averages of the double ratio over the entire p_{miss} range of each shell.[1] The fact that p_{miss}-matched super-ratios are consistent with those of Fig. 3(a), and the observed linear trend in Fig. 2 despite the points not being ordered by p_{miss}, further suggest that this is a density-dependent phenomenon.

In-medium proton modifications. The first investigation of polarization transfer sensitivity to possible density dependent in-medium modification of nucleon form factors was carried out by Kelly [1]. This was followed by several polarization-transfer experiments. Measurements of the ^{4}He$(\vec{e}, e'\vec{p}\,)$ reaction, performed both at MAMI [18] and at JLab [19,20], favored the calculations that included medium modifications models [21]. Two models were considered: the chiral quark soliton (CQS) model [3,22] that mainly modifies valence quark contributions and the quark-meson coupling (QMC) model [4,23]. However, the same data were later described by different calculations using free-proton EM FFs [24].

We compare our results with the calculations using QMC and CQS models within the relativistic multiple scattering Glauber approximation (RMSGA) [5,25]. As suggested in Ref. [5], density-dependent in-medium modifications of the bound proton should be reflected in the super-ratio of shells A

[1]Even when considering only overlapping regions, because of varying per-bin statistical uncertainties, taking the ratio of two weighted double-ratio averages does not give the same result as a direct weighted average of the super-ratio binned in p_{miss}. This is due to the sensitivity to underlying variable changing when adding uncertainties for each bin, i.e., taking whole overlap region as one bin will produce different result than if you bin it into 6 bins because of the differences in individual shell p_{miss} distributions

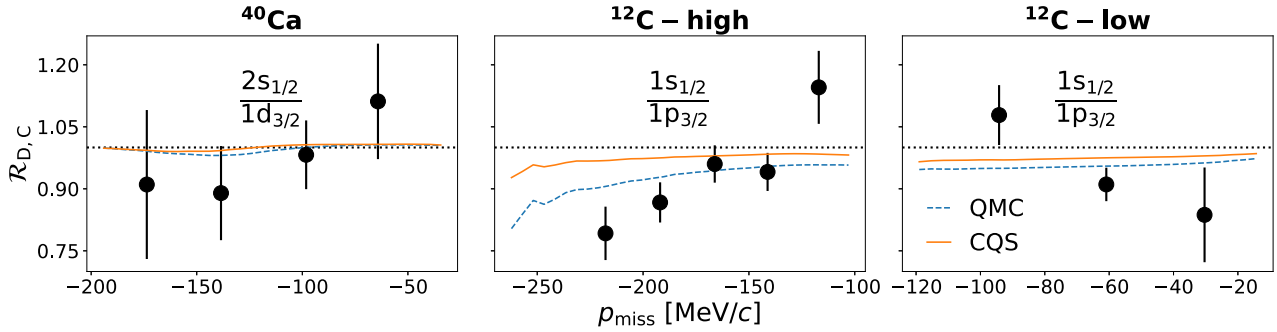

FIG. 4. The super-ratios as a function of p_{miss}. The data points show the super-ratio from Eq. (1). The lines show the super-ratios from Eq. (2) using two different models (QMC, CQS) for in-medium density-dependent modification of proton EM form factors.

and B,

$$\mathcal{R}_{\text{C}} = \frac{[(P'_x/P'_z)_{\text{A}}/(P'_x/P'_z)_{\text{B}}]_{\text{QMC,CQS}}}{[(P'_x/P'_z)_{\text{A}}/(P'_x/P'_z)_{\text{B}}]_{\text{Free}}}. \tag{2}$$

We refer to Fig. 2 in Ref. [5] and related discussion to illustrate the magnitude and density dependence of the form factor modification effects in these two models. In Fig. 3 of the same reference, it is shown how this modification is reflected in the super-ratios as a function of p_{miss}. The predictions are that the electric form factor, G_E, decreases with increasing nuclear density regardless of the model. This is unlike the magnetic form factor, G_M, which increases in the QMS model or is hardly affected within the CQS model. Combined, this results in a decrease of the form factor ratio with increasing density for both models [5]. To cover all of our kinematic settings and target nuclei we extended the original RMSGA calculations. To ensure self-consistency, the effective local nuclear density experienced by the proton from each event was also obtained in RMSGA through the procedure described in Refs. [16,26], analogous to the one that was used for calculation of RDWIA densities in previous sections.

The predicted super-ratios as a function of p_{miss} are shown for three kinematic settings of this work in Fig. 4. The super-ratio, $\mathcal{R}_{\text{C}}$, from Eq. (2) is calculated in RMSGA. The numerator is calculated using density-dependent EM FFs predicted by either QMC or CQS. The denominator is obtained by using free proton EM FFs from Ref. [27]. We compare these predictions to our *super-ratios* using Eq. (1), where data are divided by our RDWIA calculations. These super-ratios are consistent with the ones predicted by the calculations using modified density-dependent form factor. The deviations from unity are more prominent in high-p_{miss} region of ^{12}C shown in central panel of Fig. 4, where density differences between shells are the largest. The super-ratios for ^{40}Ca are about unity as the density of the shells are about equal. This observation is in line with previous analyses [20,21,28].

Conclusions. Polarization transfer to bound protons provides a sensitive tool to probe the bound proton electromagnetic form factors. However, a direct comparison of the measurements to calculations does not allow us to determine if deviations are due to many-body or in-medium modifications in the bound proton structure [6,7]. Discrepancies due to many-body effects are expected to be largely mitigated in super-ratios by comparing the double ratios of polarization-transfer data to those calculated in RDWIA for individual shells in ^{12}C ($1p_{3/2}$ and $1s_{1/2}$) and ^{40}Ca ($1d_{3/2}$ and $2s_{1/2}$).

In our present study of double and super-ratios for shells with different effective nuclear densities, we observed a systematic density-dependent deviation. We further found it to be consistent with a reduction of the EM FF ratio, G_E/G_M, for protons bound in higher density shells compared to those in lower density shells, as predicted in CQS amd QMC models. While we cannot fully exclude other density-dependent effects, past and future analyses of other polarization observables [14,15] might provide more stringent limits on FSI and other many-body effects included in various calculations.

Unlike the ratio of the transverse to the longitudinal components, which is linearly dependent on the FF ratio G_E/G_M, the transverse and longitudinal components, individually, have different dependencies on the electric and magnetic FFs. Additional high statistics data of the transfer components may yield information on the individual behavior of the EM FFs of the bound proton.

Acknowledgments. We would like to thank the Mainz Microtron operators and the technical crew for the excellent operation of the accelerator. This work is supported by the Israel Science Foundation (Grant No. 951/19) of the Israel Academy of Arts and Sciences, by the Israel Ministry of Science, Technology and Spaces, by the PAZY Foundation (Grant No. 294/18), by the Deutsche Forschungsgemeinschaft (Collaborative Research Center 1044), by the U.S. National Science Foundation (Grants No. PHY-2111050, No. PHY-2111442, and No. PHY-2239274), and by the United States-Israeli Binational Science Foundation (BS) as part of the joint program with the NSF (Grant No. 2020742). We acknowledge the financial support from the Slovenian Research Agency (research core funding No. P1-0102).

[1] J. J. Kelly, Nucleon knockout by intermediate-energy electrons, Adv. Nucl. Phys. **23**, 75 (1996).

[2] I. C. Cloët, R. Dupré, S. Riordan *et al.*, Exposing novel quark and gluon effects in nuclei, J. Phys. G: Nucl. Part. Phys. **46**, 093001 (2019).

[3] J. R. Smith and G. A. Miller, Chiral solitons in nuclei: Electromagnetic form-factors, Phys. Rev. C **70**, 065205 (2004).

[4] D.-H. Lu, A. W. Thomas, K. Tsushima, A. G. Williams, and K. Saito, In-medium electron-nucleon scattering, Phys. Lett. B **417**, 217 (1998).

[5] G. Ron, W. Cosyn, E. Piasetzky, J. Ryckebusch, and J. Lichtenstadt, Nuclear density dependence of in-medium polarization, Phys. Rev. C **87**, 028202 (2013).

[6] T. Kolar, S. Paul, T. Brecelj *et al.* (A1 Collaboration), Comparison of recoil polarization in the ^{12}C$(\vec{e}, e'\vec{p})$ process for protons extracted from s and p shell, Phys. Lett. B **811**, 135903 (2020).

[7] T. Kolar *et al.* (A1 Collaboration), Measurement of polarization transfer in the quasi-elastic ^{40}Ca$(\vec{e}, e'\vec{p})$ process, Phys. Lett. B **847**, 138309 (2023).

[8] T. Brecelj, S. J. Paul, T. Kolar *et al.* (A1 Collaboration), Polarization transfer to bound protons measured by quasielastic electron scattering on ^{12}C, Phys. Rev. C **101**, 064615 (2020).

[9] A. Meucci, C. Giusti, and F. D. Pacati, Relativistic corrections in $(e, e'p)$ knockout reactions, Phys. Rev. C **64**, 014604 (2001).

[10] S. Boffi, C. Giusti, F. d. Pacati, and M. Radici, *Electromagnetic Response of Atomic Nuclei*, Oxford Studies in Nuclear Physics Vol. 20 (Clarendon Press, Oxford, 1996).

[11] E. D. Cooper, S. Hama, and B. C. Clark, Global Dirac optical potential from helium to lead, Phys. Rev. C **80**, 034605 (2009).

[12] M. Sharma, M. Nagarajan, and P. Ring, Rho meson coupling in the relativistic mean field theory and description of exotic nuclei, Phys. Lett. B **312**, 377 (1993).

[13] J. C. Bernauer, M. O. Distler, J. Friedrich, T. Walcher *et al.* (A1 Collaboration), Electric and magnetic form factors of the proton, Phys. Rev. C **90**, 015206 (2014).

[14] T. Kolar, S. Paul *et al.* (A1 Collaboration), Measurements of the electron-helicity asymmetry in the quasi-elastic $A(\vec{e}, e'p)$ process, Phys. Lett. B **824**, 136798 (2022).

[15] S. Paul, T. Kolar, T. Brecelj *et al.* (A1 Collaboration), Measurements of the induced polarization in the quasi-elastic $A(e, e'\vec{p})$ process in non-coplanar kinematics, Phys. Lett. B **811**, 135984 (2020).

[16] J. Ryckebusch, W. Cosyn, and M. Vanhalst, Density dependence of quasifree single-nucleon knockout reactions, Phys. Rev. C **83**, 054601 (2011).

[17] T. De Forest, Off-shell electron-nucleon cross sections: The impulse approximation, Nucl. Phys. A **392**, 232 (1983).

[18] S. Dieterich *et al.*, Polarization transfer in the ^{4}He$(\vec{e}, e'\vec{p})\,^3$H reaction, Phys. Lett. B **500**, 47 (2001).

[19] S. Strauch *et al.* (Jefferson Lab E93-049 Collaboration), Polarization transfer in the ^{4}He$(\vec{e}, e'\vec{p})\,^3$H reaction up to $Q^2 = 2.6(\mathrm{GeV}/c)^2$, Phys. Rev. Lett. **91**, 052301 (2003).

[20] M. Paolone, S. P. Malace, S. Strauch *et al.* (E03-104 Collaboration), Polarization transfer in the ^{4}He$(\vec{e}, e'\vec{p})\,^3$H reaction at $Q^2 = 0.8$ and 1.3 $(\mathrm{GeV}/c)^2$, Phys. Rev. Lett. **105**, 072001 (2010).

[21] J. M. Udias, J. A. Caballero, E. Moya de Guerra, J. E. Amaro, and T. W. Donnelly, Quasielastic scattering from relativistic bound nucleons: Transverse-longitudinal response, Phys. Rev. Lett. **83**, 5451 (1999).

[22] C. V. Christov, A. Z. Gorski, K. Goeke, and P. V. Pobylitsa, Electromagnetic form-factors of the nucleon in the chiral quark soliton model, Nucl. Phys. A **592**, 513 (1995).

[23] D.-H. Lu, K. Tsushima, A. W. Thomas, A. G. Williams, and K. Saito, Electromagnetic form factors of the bound nucleon, Phys. Rev. C **60**, 068201 (1999).

[24] R. Schiavilla, O. Benhar, A. Kievsky, L. E. Marcucci, and M. Viviani, Polarization transfer in ^{4}He$(\vec{e}, e'\vec{p}\,)\,^3$H: Is the ratio G_{Ep}/G_{Mp} modified in the nuclear medium?, Phys. Rev. Lett. **94**, 072303 (2005).

[25] J. Ryckebusch, D. Debruyne, P. Lava, S. Janssen, B. Van Overmeire, and T. Van Cauteren, Relativistic formulation of Glauber theory for $A(e, e'p)$ reactions, Nucl. Phys. A **728**, 226 (2003).

[26] W. Cosyn and J. Ryckebusch, On the density dependence of single-proton and two-proton knockout reactions under quasifree conditions, Phys. Rev. C **80**, 011602(R) (2009).

[27] H. C. Budd, A. Bodek, and J. Arrington, Modeling quasi-elastic form factors for electron and neutrino scattering, arXiv:hep-ex/0308005.

[28] P. Lava, J. Ryckebusch, B. Van Overmeire, and S. Strauch, Polarization transfer in ^{4}He$(\vec{e}, e'\vec{p}\,)$ and ^{16}O$(\vec{e}, e'\vec{p}\,)$ in a relativistic glauber model, Phys. Rev. C **71**, 014605 (2005).